# Injection- and Phase-Locking Techniques for Beam Control

Robert A. York, *Member, IEEE,* and Tatsuo Itoh, *Life Fellow, IEEE*

*(Invited Paper)*

*Abstract*—**Applications of millimeter-wave radar, imaging, and communication technology requires cost-effective implementation of intelligent scanning antenna systems. Injection-locking and phase-locked-loop (PLL) techniques can be used to achieve synchronous operation of a number of antenna array elements, and allow for the manipulation of the phase distribution without additional phase-shifting circuitry, suggesting a potential for low-cost beam-scanning systems. This paper describes a number of techniques, with an assessment of some remaining technical challenges for practical implementation.**

*Index Terms*—**Beam control, injection locking,**

## I. INTRODUCTION

**A** NUMBER OF commercial opportunities are emerging in the wireless communications, imaging, and automotive electronics markets for active, "smart" antenna array systems. The technology for constructing intelligent arrays has been around for many years and has gone through considerable refinement as semiconductor device and integrated-circuit processing technology has improved. However, the emerging commercial applications have brought a number of new constraints that could make conventional phased and adaptive array techniques unattractive or prohibitively expensive. Most notably, these are: cost, size, and efficiency.

For automotive-collision avoidance or blind-spot indicators, cost is critical for market viability. Manufacturers are also reluctant to allocate more than a few square inches of surface area for possible antenna aperture, which not only makes system integration difficult, but also forces the use of higher frequencies in order to satisfy antenna beamwidth requirements. Such high frequencies stress current device technology. To further complicate matters, commercial automotive electronics must operate reliably over a wide range of temperatures and environmental conditions.

In the wireless sector, compact scanning arrays could be useful in hand-held or mobile systems to reduce power consumption through "adaptive power control," whereby the array alternates between a low-gain "search" mode and a high-gain "acquisition" mode, much like a tracking radar system. In the high-gain mode, the array has a high directivity, which requires less power for effective communication, and also reduces the susceptibility to interference when receiving. Compact scanning systems could also be used for mobile satellite links, which also require high-directivity antennas. However, these wireless applications will likely suffer the same constraints as the automotive radar electronics.

Principles of conventional phased arrays are well known. Typically coherence is maintained between array elements using a single source distributed to every array element through a corporate feed network. Separate phase shifters are required at each element, each of which requires biasing and multiple control wires. This is illustrated in Fig. 1(a). It is a challenge to collectively integrate antennas, feed networks, phase shifters, and control signals successfully into a small package due to space constraints. Components such as phase shifters can also add considerable expense to a system, depending on the size of the array and scanning requirements. At millimeter-wave frequencies, it is also difficult to generate the required output power with a single solid-state source, and this problem is compounded by large losses in the feed network and phase shifters.

Fig. 1(a) is, of course, oversimplified and shows only a transmitting system. More realistic scanning systems require transmit and receive functionality, and are most often made today using a number of active integrated transmit–receive (T/R) modules, as shown in Fig. 1(b). While all of the components in each module are standard off-the-shelf microwave and millimeter-wave components, the price of a single low-performance T/R module is typically 10–20 times what is required of the complete commercial system. This has led a number of researchers to explore techniques for combining functions of (or eliminating entirely) several of the module components.

Switched-beam, frequency-scanned, and traveling-wave phasing techniques have been suggested to solve this problem; such techniques may appeal to the widest audience of engineers since they accomplish the objective using common microwave-circuit techniques. Mechanically scanned systems
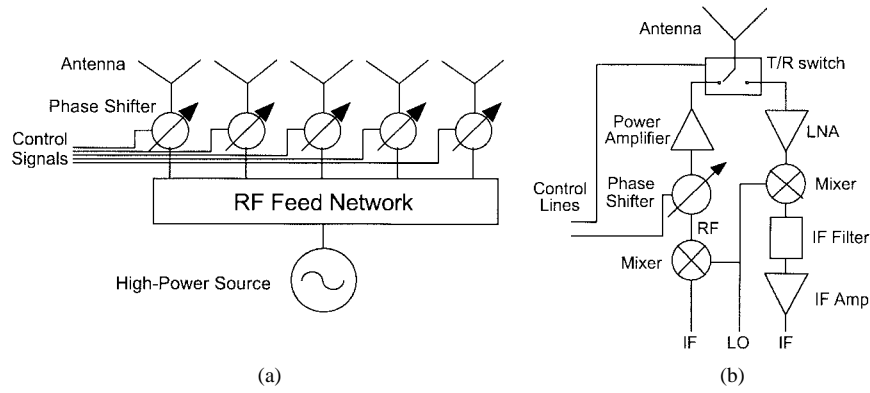
Fig. 1. (a) Conventional approach for an electronically scanned transmitter. (b) Typical T/R module used in active arrays.
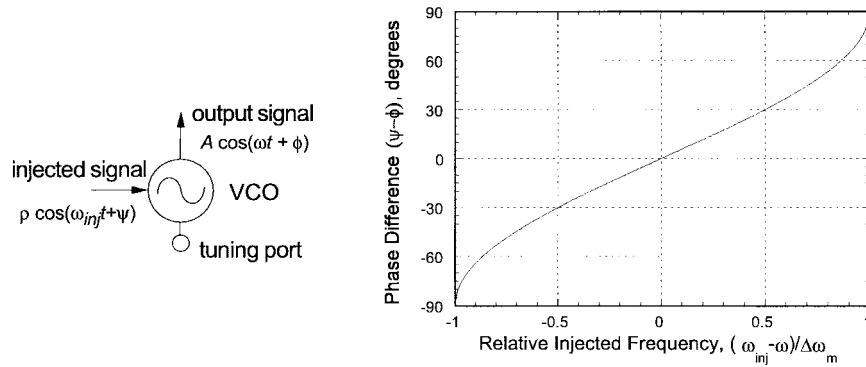


Fig. 2. Injection-locked oscillator and plot showing behavior of oscillator phase as injection frequency is varied relative to the free-running frequency.

are also a perfectly legitimate solution to the aforementioned problems, provided they can be made small and inexpensive. Mechanically scanned systems promise a large reduction in the number of RF front-end components, at the expense of introducing moving parts, which bring reliability and maintenance issues into play. Although mechanically scanned systems have limited scanning speeds, this may not be a factor in the commercial systems previously mentioned.

Less conventionally, a number of other interesting techniques have been realized using injection-locked or mutually synchronized oscillator or phase-locked-loop (PLL) arrays, and depend on the unusual phase dynamics of nonlinear oscillators to achieve the scanning objective. Coupled-oscillator arrays have been demonstrated for single-beam transmit and receive applications, and have also been demonstrated in a continuous scanning or "lighthouse" mode using a technique similar to that used in mode-locked lasers.

The common feature of all of these alternatives is that they eliminate the phase-shifter circuitry at each array element and, in some cases, the RF and control signal-distribution networks. The focus of this paper is on the injection-locked oscillator techniques, in particular, the feeding and phasing of the array elements, and not on the system integration. The proposed techniques appear to have some advantages over conventional phased arrays, but as with any real system, this typically comes at the expense of some other performance criterion; whether these are acceptable alternatives must be considered on a case-by-case basis.

## II. ADLER'S EQUATION

The practical use of nonlinear oscillators for phase control is based on the phenomenon of injection locking, sometimes called frequency entrainment. This effect has a long history dating back to observations of synchronized mechanical pendulums by Huygens [1], and has since been observed in a wide variety of self-sustained (nonlinear) biological and physical oscillators.

Using a simple single-tuned oscillator model, it can be shown [2]–[4] that the output phase of an oscillator with an injected signal is given by Adler's equation. The oscillator is then described by Adler's equation

$$\frac{d\phi}{dt} = \omega_0 - \omega_{\text{inj}} + \underbrace{\frac{\rho}{\alpha}\frac{\omega_0}{2Q}}_{\Delta\omega_m} \sin\left(\psi - \phi\right) \qquad (1)$$

where $\omega_0$ is the free-running frequency, $\alpha$ is the free-running oscillation amplitude, $Q$ is the quality-factor of the oscillator's resonant circuit, and the remaining variables are defined in Fig. 2 (see [3] and [4] for more detail). This is the key equation for injection locking, and can be generalized to multiple-oscillator systems [5]. If a steady-state solution can be found for the phase such that $d\phi/dt = 0$, this indicates that the oscillator is synchronized to the injected signal. Solving for the steady-state phase difference between the oscillator and the injected signal ($\Delta\phi = \psi - \phi_0$) gives

$$\Delta\phi = \sin^{-1}\left(\frac{\omega_{\text{inj}} - \omega_0}{\Delta\omega_m}\right) \qquad (2)$$
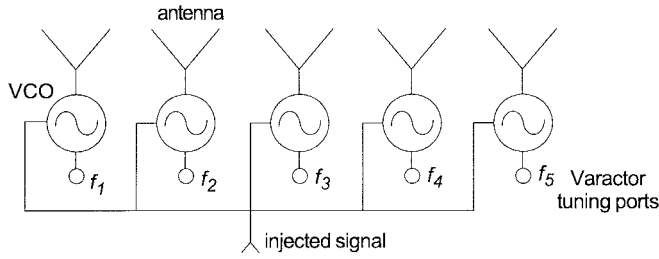
Fig. 3. Injection-locked oscillator array. Output can be scanned through electronic control of each oscillator tuning voltage.
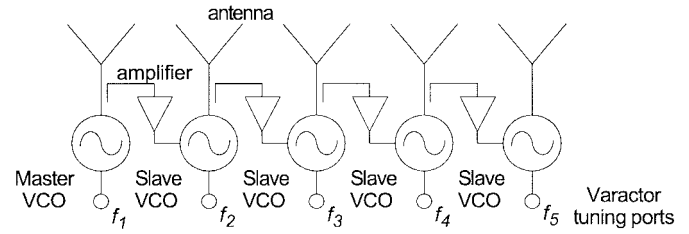


Fig. 4. Cascade of injection-locked VCO's slaved to a low-noise master oscillator. Voltage-tuning on each VCO can create a progressive phase shift along the array.

which indicates that an injection-locked solution is possible only when the injected signal frequency lies within the "locking range" of the oscillator $\omega_0 \pm \Delta\omega_m$ (note that $\Delta\omega_m$ is often referred to as the locking range, but physically represents *half* the locking range). The inverse sine function gives two possible solutions for the phase difference in this range; the correct result is found from a stability analysis. Following Section II, the phase is perturbed from its free-running state ($\phi_0$) by writing $\phi = \phi_0 + \delta\phi$, which reduces (1) to

$$\frac{d\delta\phi}{dt} = -\delta\phi \, \Delta\omega_m \, \cos \Delta\phi. \tag{3}$$

The perturbation will decay in time provided that $\cos \Delta\phi > 0$, which restricts the phase difference to the range

$$-\frac{\pi}{2} \leq \Delta\phi \leq \frac{\pi}{2}. \tag{4}$$

As the injected signal frequency is tuned over the locking range, the phase difference between the oscillator and the injected signal will vary between $\pm\pi/2$ according to (2); this is illustrated in Fig. 2. This induced phase shift suggests possible schemes for phased arrays using injection locking, which will be described later. Note that the locking range is proportional to the injected signal strength, and inversely related to the $Q$-factor. To the extent that a large locking range is desired in a practical system, low-$Q$ oscillators with large injected signal strengths are required.

## III. UNILATERAL INJECTION LOCKING

### A. Injection-Locked Arrays with a Conventional Feed

The most straightforward application of the injection-locking technique to phased arrays is shown in Fig. 3. Each array element is a self-contained voltage-controlled oscillator (VCO) that delivers its energy to an antenna. The oscillators are all slaved to a common signal (the desired output signal), which is distributed using a standard feed structure like a corporate feed network. The phase of each oscillator can be changed relative to the reference signal (and, hence, the other oscillators) by adjusting the oscillator tuning voltage (the free-running frequency) according to Fig. 2. It should be noted that oscillator arrays like this also serve as efficient power combiners; in fact, most of the techniques described in this paper have evolved from research groups investigating quasi-optical power-combining methods.

A 4 × 4 array using the topology of Fig. 3 has been reported [6], although the emphasis was on the power-combining

aspects of the array and not the possible scanning feature. Like all injection-locking techniques, this approach will be limited in bandwidth by the locking range of the oscillators, which, in turn, is related to the $Q$-factor and injected signal strength. The array topology should degrade gracefully. It may also be possible to use self-oscillating mixers as the array elements in order to combine transmit and receive functions. The external locking approach has been used in conjunction with optical signal distribution for large-aperture phased arrays by Daryoush [7] and others. This scheme is similar to that of Fig. 3, except that the RF signal is distributed to each array element via an optical carrier. A photodetector at each array element converts the optical signal to RF, which then directly injection locks a microwave oscillator.

### B. Cascade-Coupled Scanning Array

A variation of this idea which eliminates the corporate feed structure involves an injection-locked cascade, whereby each array element is slaved to the preceding element in the array. This is conceptually illustrated in Fig. 4, and has been tested experimentally for scanning applications [8]. To insure that the injection locking is unilateral, amplifiers are used between the oscillators, resulting in a nonreciprocal active coupling matrix. As a result, the dynamics of each oscillator are essentially governed by Adler's equation (1), so the relative phasing is established by adjusting the free-running frequencies of each array elements according to Fig. 2. The amplifiers increase the circuit complexity, but also help boost the signal strength for a better locking range and, hence, bandwidth. The amplifiers also are used so that only a small amount of power needs to be coupled out of each oscillator, thus, the coupler does not strongly affect the oscillator performance, and most of the oscillator power is delivered to the antenna. The extension to two-dimensional arrays is straightforward.

A 4 × 1 active antenna array was designed and tested to demonstrate this concept (see Fig. 5). The array is fabricated on Duroid substrate with a dielectric constant of 2.33 and thickness of 31 mil. Rectangular patch antennas were used in this design. Microstrip couplers are incorporated at the gate and drain ports of the FET for injection and tapping of signals, respectively. The active device (NEC 72 084) is self-biased at $V_{ds} = 3$ V and $I_{ds} = 30$ mA. The free-running frequency of the oscillators can be tuned independently through the drain bias, but this also affects the output power. The amplifier used in this circuit is an HP MGA 64 135. It has a gain of 9 dB with an isolation of 26 dB. The oscillators operate at 5.8 GHz,
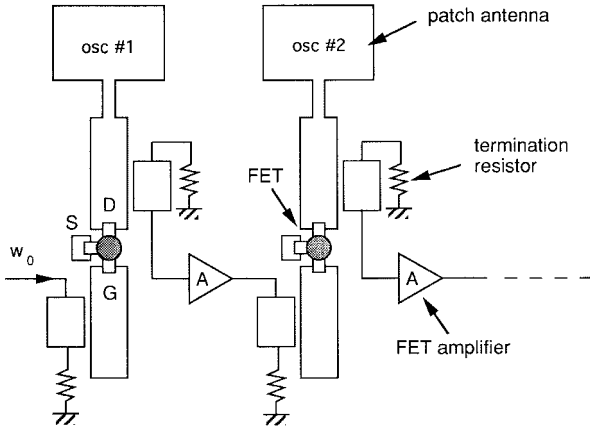
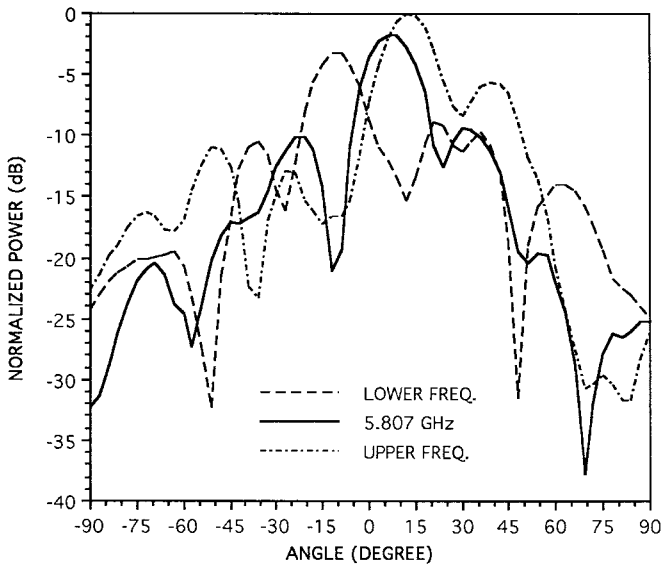Fig. 5. Illustration of the unilateral injection-locked array prototype.



Fig. 6. Beam patterns for an experimental unilateral injection-locking system.



Fig. 7. Optically fed unilateral injection-locking system.

with a tuning range of approximately 30 MHz. The antenna elements are placed 0.89 $\lambda_0$ apart, where $\lambda_0$ is the free-space wavelength at 5.8 GHz. The measured pattern is shown in Fig. 6. With this spacing, the theoretical scan angle is 33° and the measured scan angle is about 24°. The scanned pattern is asymmetrical with varied peak transmitted power. These discrepancies are partly due to the difficulty in achieving band-edge injection locking and uncompensated coupling phase. However, the main cause of the difference in peak power is due to the difference in drain voltages of the oscillators. This is a compromise for circuit simplicity.

One feature of all injection-locked arrays is that the oscillators will roughly assume the noise properties of the master oscillator or reference signal, even if the oscillators themselves are quite noisy. However, the coupling network will have some influence on the specific noise reduction. The array in Fig. 4 will collectively have a low phase noise as long as the injected signal is derived from a "quiet" source. However, an analysis shows a slight noise degradation as the number of oscillators increases [9].
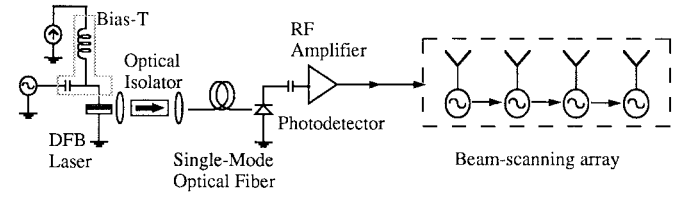
In the circuit of Fig. 4, the external reference signal is injected using a coaxial cable. However, for remoting of microwave systems, this reference signal may be better transmitted via an optical link, due to low loss, compactness, and immunity to electromagnetic interference of the optical fiber. The schematic diagram of the conceptual optical-link system is shown in Fig. 7. The system consists of the following four subcircuits:

1) laser diode to convert the RF signal to an intensity-modulated optical signal;
2) length of fiber to carry the modulated lightwave to the active antenna;
3) high-speed photodetector/amplifier subcircuit to recover the RF signal from the optical signal;
4) active antenna array, which is fed by the recovered RF signal for injection locking.

RF-to-optical conversion is achieved by direct modulating a distributed feedback (DFB) laser. By superimposing the RF reference signal on the laser drive current, the light intensity can be modulated accordingly. The laser is a multiquantum well (MQW) InGaAs-InGaAsP DFB laser. It is index guided by a buried heterostructure with an active region width of 1 mm. The DFB laser is mounted on an HP83041C microcircuit package with wire bonding. To convert the RF signal into an optical signal, the DFB laser is prebiased at a dc current such that the frequency response peaks at the RF operating frequency. The RF reference signal is then superimposed on the biasing current through a bias tee. The modulated optical signal is then coupled by lenses into a 3-m-long standard single-mode fiber (SMF) with a core diameter of 9 mm. The temperature of the DFB laser is maintained at 15 °C. To avoid reflections between the two lenses, an optical isolator is inserted between them. At the other end of the SMF, a high-speed HP 83440D photodetector is used to detect and reconvert the optical signal into an RF signal.

Finally, an amplifier is used to increase the power level to a sufficient level for injection locking before pumping the signal into the active antenna system. Measured results [10] for this system are similar to the coaxial-fed system with a scan angle of 21°. The discrepancy in scan angle between the above-mentioned systems is mainly due to the higher system noise level in the optical-link system.

### C. Beam-Switching Array

In radar and anti-car collision applications, beam switching is used for tracking purposes. In a beam-switching array, a difference pattern in the azimuth and elevation planes can be synthesized only if there are an even number of row
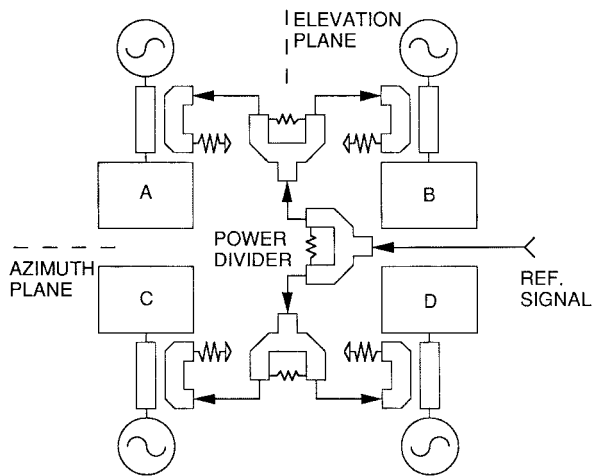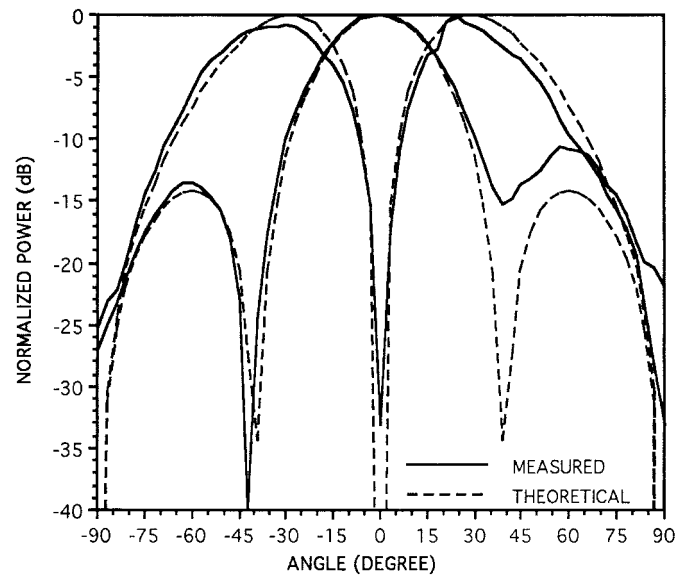
Fig. 8.  Four-quadrant beam-switching system using injection-locking techniques for phase control.



(a)



(b)

Fig. 9.  Representative patterns for the beam-switching system of Fig. 8 in (a) azimuth and (b) elevation.

and column elements. When all four quadrants are fed in-phase with respect to each other, a sum pattern is formed in azimuth and elevation. However, when quadrants I and III are kept in-phase at $+90°$ with respect to the reference signal, and quadrants II and IV are kept in phase at $-90°$, difference and sum patterns are formed in the azimuth and elevation planes, respectively. Different combinations of phase relationship resulting in various patterns in both planes can be synthesized and are described in [11].
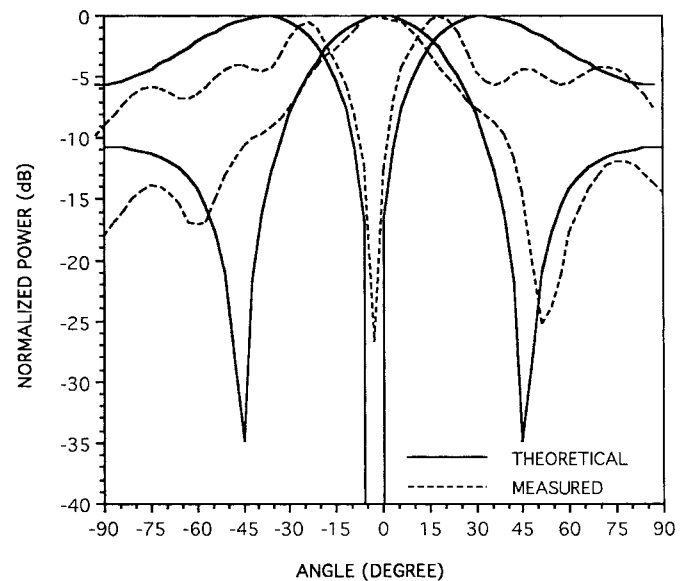
A $2 \times 2$ active antenna array, designed on a Duriod substrate with a dielectric constant of 2.33 and a thickness of 31 mil is used to demonstrate the concept. The schematic diagram of the array is shown in Fig. 8. Only one coupler at the drain of the FET is integrated to date for injection locking. A Wilkinson power divider is used for the power division of the injected signal. The reflection coefficients of all three ports are better than 20 dB. The maximum power and phase imbalance and isolation between the two output ports are 0.2 dB and 1.5°, and 18 dB, respectively. Injection locking is controlled by the level of coupling in the coupler and isolation between the output ports of the power divider.

The upper and the lower quadrants are fed on the opposite sides of their respective patches, resulting in 180° excitation. This is due to space constraint and circuit stability. The critical performance of this circuit lies in its ability to have a deep and well-defined null at broadside for the difference pattern. A difference pattern is formed when the free-running frequencies of the oscillators are tuned to the injected signal. This is a very stable operating point. It was noted that instability results when the free-running frequency is tuned to that of the locking band edge [12]. Thus, the free-running frequencies are tuned close, but not at the edge of the band. This caused the sum pattern to have a lower power level with possible offset in the position of the main beam. This circuit is designed with emphasis in a well-defined null in the difference pattern. However, due to space constraint, such implementation is available only in the elevation plane.

The active antenna array was measured for all permutations of sum and difference patterns in azimuth and elevation. Note

that when establishing the phase relationship, the antennas are fed on the opposite side of their respective patch antennas, which can introduce a 180° phase change. A comparison is made with the theoretical patterns calculated using a simplified model [13]. The oscillating frequency is about 6.62 GHz and can be varied independently by at least 40 MHz via their respective drain bias. The measured sum and difference patterns in the azimuth plane are shown in Fig. 9(a). The measured effective radiated power (ERP) of the sum pattern is 30 dBm. The null of the difference pattern at broadside is better than $-28$ dB, and there is asymmetry in the difference pattern. This is due to the difference in the output power level of the oscillator for different free-running frequency. Both patterns agree well with the theoretical results. In the elevation plane, the sum and difference patterns are shown in
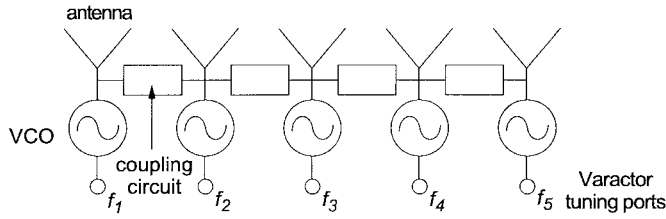
Fig. 10. Bilaterally coupled oscillator system, also known as "interinjection-locking" or mutual synchronization.
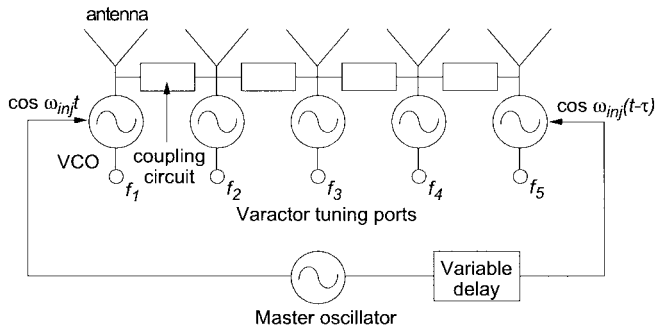


Fig. 11. Scanning approach proposed by Stephan, whereby a phase difference between externally injected signals is divided uniformly across the array due to the bilateral coupling.

Fig. 9(b). The null in the difference pattern is better than $-30$ dB. However, these plots do not match the theoretical results very well. This may be due to radiation from the rest of the circuit. Nevertheless, in general, the patterns agree well.

## IV. BILATERAL INJECTION-LOCKING OR MUTUAL SYNCHRONIZATION

A less obvious, but intriguing, extension of the injection-locking concept is an array of mutually synchronized oscillators, such as illustrated in Fig. 10. Each oscillator is bilaterally coupled to neighboring array elements. This system was first proposed by Stephan [14], who described the system as "interinjection-locked" oscillators. Mutual coherence is achieved via the injection-locking process, but the steady-state phase relationships are more difficult to calculate since each oscillator depends on its neighbors' phase. A nonlinear system of simultaneous equations must be solved to determine the self-consistent phase relationships [5]. However, in certain cases, the equations can be linearized and solved for the necessary conditions to produce the phase progressions required for beam scanning. This has led to some interesting approaches.

### A. Stephan's Scanning Approach

Stephan's array, shown in Fig. 11 [14], [15], is a nearest neighbor bilaterally coupled, or "interinjection-locked" array, with external signals injected at opposite ends of the array. The two injected signals are coherent with a variable relative phase, which is implemented by splitting the signal from a common master oscillator and delaying one of the channels. Stephan found the interesting property that, under certain conditions, the phase difference between the two injected signals is divided uniformly along the array to produce a

constant phase progression. This can be explained using a modified version of Adler's equation for multiple coupled oscillator systems with external locking signals. Assuming the oscillation amplitudes are all essentially the same, it can be shown [4] that such systems are described by

$$\frac{d\phi_i}{dt} = (\omega_i - \omega_{inj}) - \frac{\epsilon\omega_i}{2Q}[\sin(\phi_i - \phi_{i-1}) + \sin(\phi_i - \phi_{i+1})]$$
$$+ \frac{\omega_i\rho_i}{2Q}\sin(\psi_i - \phi_i) \quad (5)$$

for $i = 1, \cdots, N$, where $\omega_i$ and $\phi_i$ are the free-running frequency and phase of the $i$th oscillator, $\epsilon$ is the coupling strength relative to the oscillator amplitude, $\rho_i$ is the injection signal strength at the $i$th oscillator relative to the oscillation amplitude, and $\psi_i$ is the phase of the injected signal. It is implicitly understood that any terms containing subscripts 0 or $N+1$ are ignored. For the configuration of Fig. 11, we have only two injected signals, so

$$\rho_i = \begin{cases} \rho, & i = 1 \text{ or } i = N \\ 0, & \text{otherwise.} \end{cases} \quad (6)$$

We will assume that the strength of the injected signal is the same as the strength of the coupling between oscillators $\rho = \epsilon$. Therefore, a constant phase progression given by $\phi_i - \phi_{i-1} = \Delta\phi$ is a valid solution to (5) provided that

$$\omega_{inj}$$
$$= \begin{cases} \omega_1 + \Delta\omega_m[\sin\Delta\phi + \sin(\psi_1 - \phi_1)], & i = 1 \\ \omega_i, & 2 \leq i \leq N-1 \\ \omega_N + \Delta\omega_m[-\sin\Delta\phi + \sin(\psi_N - \phi_N)], & i = N \end{cases}$$
$$(7)$$

where $\Delta\omega_m = \epsilon\omega_i/2Q$, which is a constant for all $i$ to first order. Assuming all of the free-running frequencies are the same as the injected signal frequency $\omega_i = \omega_{inj}$, then we must have $\phi_1 - \psi_1 = \Delta\phi$ and $\psi_N - \phi_N = \Delta\phi$. We can assume that one of the injected signals establishes a common phase reference, which we will take as $\psi_1 = 0$, which means that $\phi_i = i\Delta\phi$, and, therefore,

$$\psi_N = (N+1)\Delta\phi. \quad (8)$$

In other words, a constant phase progression is a solution to (5) provided that the injected signals have a relative phase difference given by (8), which implies that the phase difference between the injected signals is divided uniformly along the array. For sinusoidal signals, the largest unambiguous relative phasing between the two injected signals is $\psi_N = \pi$, which implies an interelement phase shift of $\Delta\phi = \pi/(N+1)$.

This result must be checked for stability. This is done in [4] and again leads to the constraint (4). As with all simple injection-locked systems, the maximum phase shift between adjacent oscillators is $\pm\pi/2$, which for an array with $\lambda_0/2$ spacing gives a maximum scan angle of $\pm30°$ off broadside.

Morgan and Stephan [16] reported a four-element $X$-band prototype using the configuration of Fig. 11, with microstrip Gunn diode oscillators and tapered-slot antennas. The measured output phase versus injected control phase difference ($\psi_N - \psi_1$) showed good qualitative agreement with the simple
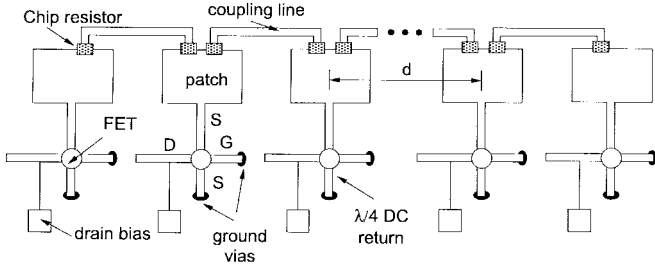
Fig. 12.  Illustration of a nearest neighbor coupling scheme using MESFET oscillators feeding patch antennas. The coupling lines are nominally one-wavelength long.



(a)



(b)

Fig. 13.  Representative measured patterns for the array of Fig. 12. (a) A nearly broadside pattern was obtained with all the elements set to approximately the same free-running frequency. (b) A scanned pattern in the range of $-15°$ to $+30°$ off broadside was obtained by symmetrically detuning the end oscillators.

theory described above. Departures from a perfect uniform phase progression and a linear dependence on the injected phase difference can be explained by including many of the effects neglected in the above analysis such as nonuniform oscillator free-running parameters, amplitude dynamics, and nonuniform loading and coupling of the array elements.

*B. Scanning by Edge Detuning*

From (5), we see that the phase distribution in the steady-state strongly depends on the distribution of free-running frequencies, or oscillator "tunings," as expected from basic injection-locking theory. We now ask, under what tunings conditions can a uniform phase progression be established on the array without any external locking signals present. For beam scanning, a constant progressive phase shift of $\Delta\phi$ is required, represented again as

$$\phi_i - \phi_{i-1} = \Delta\phi, \qquad i = 2, \cdots, N.$$
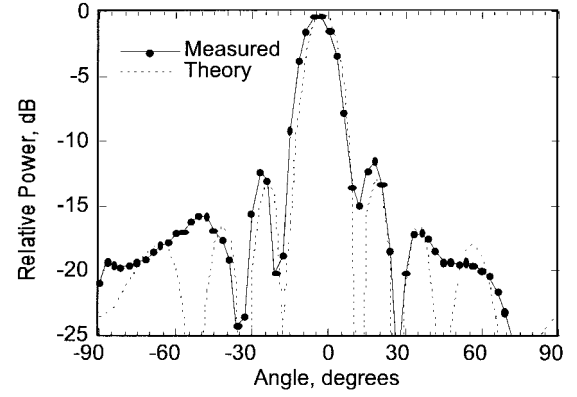
Substituting this condition into (5) in the steady state leads to a set of conditions on the free-running frequencies

$$\omega_i = \begin{cases} \omega_0 + \Delta\omega_m \sin\Delta\phi, & \text{if } i = 1 \\ \omega_0, & \text{if } 1 < i < N \\ \omega_0 - \Delta\omega_m \sin\Delta\phi, & \text{if } i = N \end{cases} \qquad (9)$$
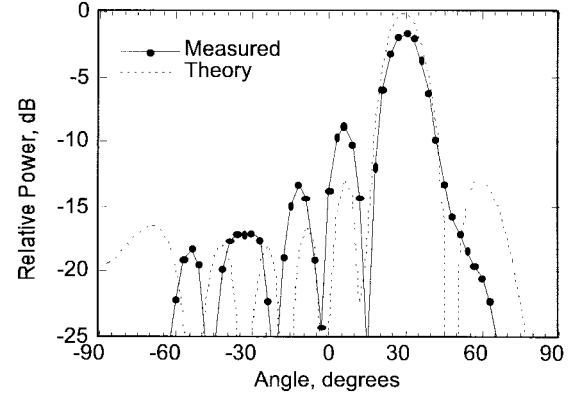
where $\omega_0$ is the desired steady-state synchronized frequency and $\Delta\omega_m = \varepsilon\omega_0/2Q$ is the locking range. This indicates that a constant phase shift can be programmed by slightly detuning only the end elements of the array in opposite directions. This appears to be the key advantage of this technique over the unilateral injection-locked oscillators: only peripheral array elements need to be voltage controlled.

Again, a stability analysis limits the range of allowed phase shifts to $\pm\pi/2$. This simplified analysis serves to introduce the beam-scanning concept, but in reality, the dynamics are complicated by many factors that have been left out of (5), such as amplitude dynamics and nonuniformities, frequency-dependent coupling networks, nonnearest neighbor interactions, nonuniform tuning profiles of the VCO's, and frequency-dependent device characteristics. Some of these issues are considered more carefully in [4].

This beam-scanning technique has been verified experimentally. An eight-element array was constructed using a coupling topology like that shown in Fig. 12 [19]. The array was designed to operate at 8.4 GHz and featured an element separation of one half-wavelength. The maximum beam-scan
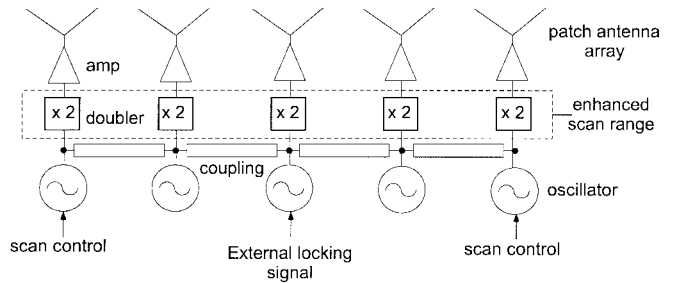


Fig. 14.  The scan range of the coupled-oscillator system can be effectively doubled using a set of frequency multiplers between the oscillator outputs and the antennas.

range for this array was, therefore, $\pm30°$ off broadside. The array was comprised of eight VCO's, each of which used an NEC 900 276 packaged GaAs MESFET (two parasitic elements are shown in the figure). The oscillator was designed in a feedback topology using a single-device amplifier with a tunable microstrip patch antenna in the feedback path. This varactor tuned patch served as a resonant load for the amplifier [20]. By adjusting the varactor bias, the free-running frequency of each oscillator was variable over a range of 150 MHz.

The ERP of the array was measured to be 8.5 W at 8.43 GHz. Fig. 13(a) illustrates a typical broadside pattern,
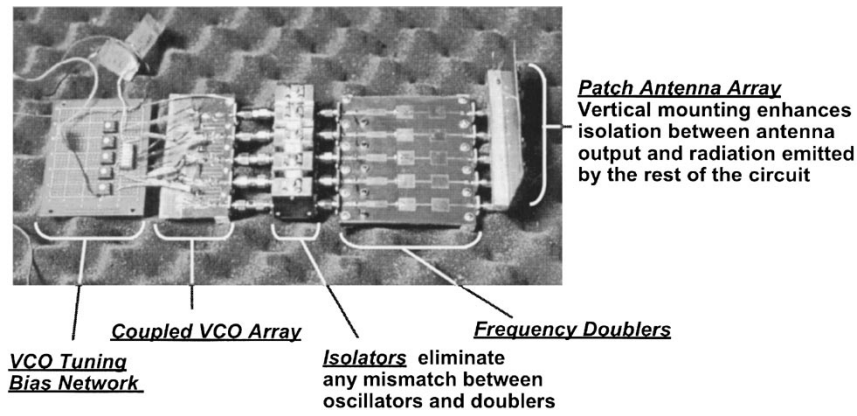
Fig. 15. Photograph of a prototype array using MESFET frequency doublers to extend the operating frequency and scan range. The VCO array was similar to that shown in Fig. 12, and operated at 4 GHz. The antenna spacing was a half-wavelength at the output frequency of 8 GHz.

which was obtained when the free-running frequencies of the oscillators in the array were set to 8.45 GHz. Varying the end-element tunings in the manner predicted by (9), it was possible to scan the array from $-15°$ to $+30°$ off broadside; a representative scanned pattern in shown in Fig. 13(b). This scanning range indicates that progressive phase shifts were achieved in the range of $-47° \leq \Delta\theta \leq +90°$. A maximum phase difference of $630°$ was established between the first and last elements in the array. That the scan range is centered away from broadside is consistent with a nonzero coupling phase angle. This could be a result of a propagation delays through the chip resistors in the coupling network, which was not accounted for in this first-iteration design. Since the patterns closely resemble the theoretical patterns for a patch array, the directivity could be accurately estimated from theory, yielding a total radiated power of over 1 W for this array. This is consistent with the expected output power from the collection of devices.

## C. Enhancements

One apparent limitation of the injection-locked or coupled-oscillator topologies (for some applications) is the limited range of phase shifts that can be synthesized. This could be improved by introducing a frequency-doubler circuit after each oscillator, as suggested in Fig. 14, which effectively doubles the interelement phase shift. Despite additional circuit complexity, this technique has some additional benefits: the oscillators can be designed at a lower frequency (half the desired output frequency), which is useful because oscillators are sensitive to parasitic reactances, and also because oscillator design is simpler when the device has high gain, which is more easily achieved at lower frequencies. The range of oscillator tuning required to achieve a given scan range is also significantly reduced, which is advantageous since operation of the array near the locking band edge is undesirable due to increased phase noise, reduced modulation range, and increased sensitivity to environmental disturbances.

FET-based doublers also provide a useful measure of isolation between the oscillator and load, so a stable broadband load impedance is presented to the oscillators, with the possibility of conversion gain (although this rules out quasi-
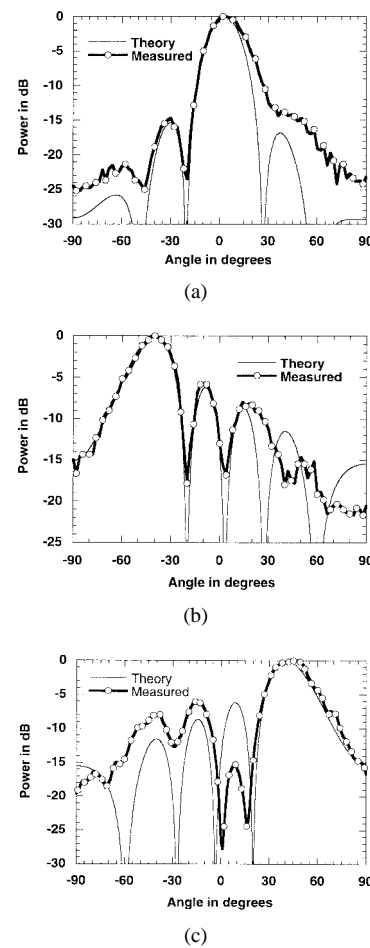


(a)



(b)



(c)

Fig. 16. Representative beam patterns for the FET-double array with free-running frequencies adjusted for (a) broadside beamforming. (b) $-40°$ scan angle. (c) $+40°$ scan angle.

optical injection locking). A five-element prototype array using FET doublers has been demonstrated at $X$-band [21], and is shown in Fig. 15. The VCO array was similar to that described earlier, operating at 4 GHz. Representative beam patterns are shown in Fig. 16. Based on these patterns and fitting to elementary array theory, a total interelement phase variation of $\approx 260°$ was inferred. That this did not result in a wider scan range is a result of the use of patch radiators.
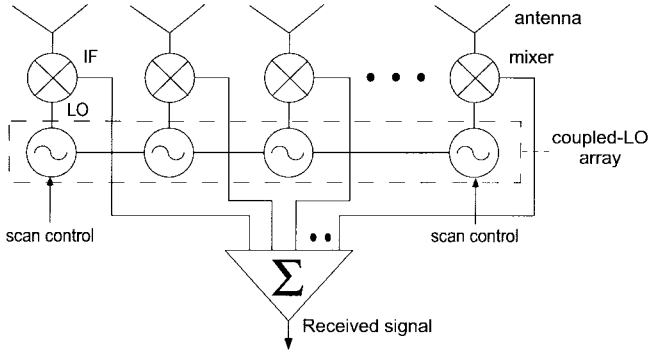
Fig. 17. The scanning technique can also be implemented in a receive mode by using the oscillator array as a set of coupled local oscillators and appropriately summing the downconverted outputs.



Fig. 18. A conceptual coupled PLL array, which mimics the behavior of the coupled-oscillator systems.

Lowering the phase noise of the oscillator arrays will be important, particularly in a frequency-doubled array since the oscillator noise is also doubled. Low noise can be achieved by injecting a stable reference signal (which could be modulated) into a *center* element of the array, as shown in Fig. 14. This has been analyzed in detail in [22].

Injection locking the array to a reference source is also related to the question of modulation. The approach has inherently narrow instantaneous frequency response and, hence, would probably be restricted to narrow-band communications. However, it *is* well suited to broad-band frequency-modulated continuous-wave (FMCW) radar or imaging configurations, in which case the output frequency of the array must be linearly swept over a certain bandwidth. For best resolution, wide bandwidths are required. At millimeter wavelengths, it is significantly easier to achieve a certain absolute bandwidth since the carrier frequency is so much higher. In the coupled-oscillator array, this could be accomplished by linearly sweeping the tuning voltage to each array element at the same rate. The scanning technique depends only on the instantaneous difference in oscillator free-running frequencies, provided the rate is slow compared to the carrier (which is usually the case) and, hence, should not be affected by an FMCW waveform, at least to first order.

The edge-detuned scanning configuration can also be employed in a receiving application [23]. This is accomplished by using the scanning oscillator array as the local oscillator for a set of mixers, as suggested in Fig. 17. Using early array prototypes and some commercial packaged mixers, this concept was tested by first measuring the scanning properties in the transmit mode (oscillators coupled directly to antennas), followed by the receive mode. As expected [23], identical scan ranges and patterns were observed in each case. It may be possible to merge the transmit and receive functions, especially for FMCW imaging arrays, by making each array element a self-contained FMCW transmitter and receiver, with each array element coupled to its neighbors. Alternatively, each array element could be a self-oscillating mixer. These concepts have not yet been tested.

## V. PLL TECHNIQUES

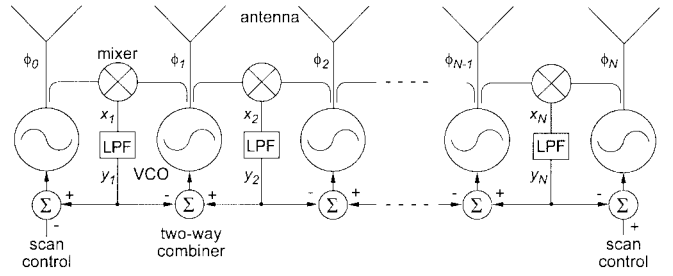Phase dynamics in a simple zeroth-order PLL circuit are also governed by an equation resembling Adler's equation for injection locking. As a result, the injection-locked systems and techniques described above can all be reproduced by using PLL techniques, at the expense of some added complexity in the circuit design. There is also a strong potential for improvement in both bandwidth and noise performance using PLL's. PLL techniques have also been employed for creating mode-locked oscillator systems for pulsed applications [24].

A coupled-PLL array system for beam scanning is shown schematically in Fig. 18. This is described in [25] and is similar to work described in [26]. We will show that this system is directly analogous to the coupled-oscillator systems described above and yields scanning properties by edge detuning in a similar fashion, but with a significantly larger locking/capture range. Using the notation in the figure, we can write the following equations relating the signals in each part of the individual "loops": for the VCO, we have

$$\omega + \frac{d\phi_n}{dt} = \omega_n[1 + C_1(y_{n+1} - y_n)], \qquad n = 0, \cdots, N \quad (10)$$

where $C_1$ is a constant describing the tuning sensitivity of the VCO, in units of 1/V, and $\omega_n$ is again the free-running frequency of the VCO, in this case, corresponding to the oscillation frequency in the absence of a tuning voltage. Here, $N + 1$ is the number of oscillators, and $y_0 = y_{N+1} = 0$. The mixer or phase detector is described by

$$x_n = C_2 \sin(\phi_n - \phi_{n-1}), \qquad n = 1, \cdots, N \quad (11)$$

where $C_2$ is a constant describing the conversion loss (also related to the VCO output amplitude), in the units of volts; the low-pass filter (LPF), which could represent an active amplifier, is described by

$$\frac{dy_n}{dt} = \omega_f y_n + \omega_f x_n, \qquad n = 1, \cdots, N \quad (12)$$

where $\omega_f$ is the filter cutoff (any gain in the loop could be included in the constant $C_2$). As with the coupled-oscillator analysis, we can remove the common steady-state frequency $\omega$ by relative phases and tunings. Letting $\Delta\phi_n = \phi_n - \phi_{n-1}$ and $\Delta\beta_n = \omega_n - \omega_{n-1}$, (10) and (12) can be approximated by

$$\frac{d\Delta\phi_n}{dt} = \Delta\beta_n + C_1\omega_0[y_{n+1} - 2y_n + y_{n-1}] \quad (13)$$

$$\frac{dy_n}{dt} = -\omega_f y_n + \omega_f C_2 \sin(\Delta\phi_n) \quad (14)$$

where $n = 1, \cdots, N$ and $\omega_0$ is an average tuning. The next step is to find the steady-state points which satisfy

$$y_n = C_2 \sin(\Delta\phi_n) \quad (15)$$

$$\Delta\omega_n = - C_1\omega_0[y_{n+1} - 2y_n + y_{n-1}]. \qquad (16)$$

The free-running frequencies must, therefore, satisfy

$$\Delta\beta_n = -C_1 C_2 \omega_0 [\sin(\Delta\phi_{n+1}) - 2\sin(\Delta\phi_n) + \sin(\Delta\phi_{n-1})]. \qquad (17)$$

For a uniform phase progression, this is identical in form to (9). The coupled PLL array system behaves essentially the same as a coupled-oscillator system. The product $C_1 C_2$ is essentially the loop gain of the PLL, and we can see that $C_1 C_2 \omega_0$ plays the role of the locking bandwidth. To the extent that we can increase the loop gain (by including an amplifier in the path of the LPF), we can enormously increase the locking range compared with a similar injection-locked array.

## VI. CONCLUSIONS

This paper has reviewed several techniques for beam control in antenna arrays using injection-locking and phase-locking methods. Variations and extensions of the topics presented are currently under investigation by several groups, and may simplify commercial scanning systems and reduce cost by eliminating phase shifters and other components. The technology is still relatively new, and it is not clear whether the benefits of the new techniques outweigh the new difficulties that are introduced. In the near term, these new approaches could find use in low-cost low-performance millimeter-wave imaging systems, as they are inherently suited to the FMCW technique. As the understanding of coupled-oscillator systems improve, it may well be possible to achieve high performance with the proposed methods. Most likely, the techniques based on PLL circuits will be most useful in practice.

## ACKNOWLEDGMENT

## REFERENCES

[1] A. E. Siegman, *Lasers.* Mill Valley, CA: Univ. Sci. Books, 1986.
[2] R. Adler, "A study of locking phenomena in oscillators," *Proc. IRE,* vol. 34, pp. 351–357, June 1946 (reprinted *Proc. IEEE,* vol. 61, pp. 1380–1385, Oct. 1973).
[3] K. Kurokawa, "Injection-locking of solid-state microwave oscillators," *Proc. IEEE,* vol. 61, pp. 1386–1409, Oct. 1973.
[4] J. J. Lynch, H. C. Chang, and R. A. York, "Coupled-oscillator arrays and scanning techniques," in *Active and Quasi-Optical Arrays for Solid-State Power Combining,* R. York and Z. Popović, Eds. New York: Wiley, 1997, ch. 4.
[5] R. A. York, "Nonlinear analysis of phase relationships in quasi-optical oscillator arrays," *IEEE Trans. Microwave Theory and Tech.,* vol. 41, pp. 1799–1809, Oct. 1993.
[6] J. Birkeland and T. Itoh, "A 16-element quasi-optical FET oscillator power combining array with external injection locking," *IEEE Trans. Microwave Theory and Tech.,* vol. 40, pp. 475–481, Mar. 1992.
[7] A. S. Daryoush, "Optical synchronization of millimeter-wave oscillators for distributed architectures," *IEEE Trans. Microwave Theory and Tech.,* vol. 38, pp. 467–476, May 1990.
[8] J. Lin, S. T. Chew, and T. Itoh, "A unilateral injection-locking type active phased array for beam scanning," in *IEEE MTT-S Int. Microwave Symp. Dig.,* San Diego, CA, May 1994, pp. 1231–1234.
[9] H.-C. Chang, X. Cao, U. Mishra, and R. A. York, "Phase noise in coupled oscillators: Theory and experiment," *IEEE Trans. Microwave Theory and Tech.,* vol. 45, pp. 604–615, May 1997.
[10] S. T. Chew *et al.,* "An active phased array with optical input and beam-scanning capability," *IEEE Microwave Guided Wave Lett.,* vol. 4, pp. 347–349, Oct. 1994.
[11] S. T. Chew and T. Itoh, "A 2 × 2 beam-switching active antenna array," in *IEEE MTT-S Int. Microwave Symp. Dig.,* Orlando, FL, May 1995, pp. 925–928.
[12] P. S. Hall, I. L. Morrow, P. M. Haskins, and J. S. Dahele, "Phase control in injection locked microstrip active antennas," in *IEEE MTT-S Int. Microwave Symp. Dig.,* San Diego, CA, May 1994, pp. 1227–1230.
[13] C. A. Balanis, *Antenna Theory, Analysis and Design.* New York: Wiley, 1982.
[14] K. D. Stephan, "Inter-injection-locked oscillators for power combining and phased arrays," *IEEE Trans. Microwave Theory Tech.,* vol. MTT-34, pp. 1017–1025, Oct. 1986.
[15] K. D. Stephan and W. A. Morgan, "Analysis of inter-injection-locked oscillators for integrated phased arrays," *IEEE Trans. Antennas Propagat.,* vol. AP-35, pp. 771–781, July 1987.
[16] W. A. Morgan and K. D. Stephan, "An $X$-band experimental model of a millimeter-wave interinjection-locked phased array system," *IEEE Trans. Antennas Propagat.,* vol. 36, pp. 1641–1645, Nov. 1988.
[17] P. Liao and R. A. York, "A new phase-shifterless beam scanning technique using arrays of coupled oscillators," *IEEE Trans. Microwave Theory and Tech.,* pp. 1810–1815, Oct. 1993.
[18] _____, "A six-element scanning oscillator array," *IEEE Microwave Guided Wave Lett.,* vol. 4, pp. 20–22, Jan. 1994.
[19] _____, "A 1-W $X$-band power-combining array using coupled VCO's," in *IEEE MTT-S Int. Microwave Symp. Dig.,* San Diego, CA, May 1994, pp. 1235–1238.
[20] _____, "A varactor-tuned patch oscillator for active arrays," *IEEE Microwave Guided Wave Lett.,* vol. 4, pp. 335–337, Oct. 1994.
[21] A. Alexanian, H. C. Chang, and R. A. York, "Enhanced scanning range in coupled oscillator arrays utilizing frequency multipliers," in *IEEE AP-S Symp. Dig.,* Newport Beach, CA, 1995, pp. 1308–1310.
[22] H.-C. Chang, X. Cao, M. J. Vaughan, U. K. Mishra, and R. A. York, "Phase noise in externally injection-locked oscillator arrays," *IEEE Trans. Microwave Theory Tech.,* vol. 45, pp. 2035–2042, Nov. 1997.
[23] X. Cao and R. A. York, "Coupled oscillator scanning technique for receiver applications," in *IEEE AP-S Symp. Dig.,* Newport Beach, CA, 1995, pp. 1311–1314.
[24] J. J. Lynch and R. A. York, "Mode-locked arrays of coupled phase-locked loops," *IEEE Microwave Guided Wave Lett.,* vol. 5, pp. 213–215, July 1995.
[25] J. J. Lynch, "Analysis and design of systems of coupled microwave oscillators," Ph.D. dissertation, Dept. Elect. Comput. Eng., Univ. California at Santa Barbara, Santa Barbara, CA, Jan. 1996.
[26] R. D. Martinez and R. C. Compton, "Electronic beamsteering of active arrays with phase-locked loops," *IEEE Microwave Guided Wave Lett.,* vol. 4, pp. 166–168, June 1994.

**Robert A. York** (S'85–M'92) received the B.S. degree in electrical engineering from the University of New Hampshire, Durham, in 1987, and the M.S. and Ph.D. degrees in electrical engineering from Cornell University, Ithaca, NY, in 1989 and 1991, respectively.

He is currently an Associate Professor of electrical and computer engineering at the University of California at Santa Barbara (UCSB), where his group is currently involved with the design and fabrication of novel microwave and millimeter-wave circuits, microwave photonics, high-power microwave and millimeter-wave modules using spatial combining and wide-bandgap semiconductor devices, and application of ferroelectric materials to microwave and millimeter-wave circuits and systems.

Dr. York received the U.S. Army Research Office Young Investigator Award in 1993, and the Office of Naval Research Young Investigator Award in 1996.


**Tatsuo Itoh** (S'69–M'69–SM'74–F'82–LF'94), for photograph and biography, see this issue, p. 1900.